JOURNAL OF SOLID STATE CHEMISTRY 51, 355–363 (1984)

Conductivity and Thermogravimetric Studies of $HTi_2NbO_7 \cdot 2H_2O$ and $CsTi_2NbO_7$

MISRI LAL* AND ARTHUR T. HOWE†

Department of Inorganic and Structural Chemistry, University of Leeds, Leeds LS2 9JT, United Kingdom

Received June 8, 1983

A detailed study was performed of the interrelationships of the lattice parameters, ionic conductivity, and infrared spectrum of $HTi_2NbO_7 \cdot 2H_2O$ as a function of dehydration. We have shown that the oxide layers in this ion-exchange compound are interspaced with water layers 2-molecules thick, providing a rare example of a bilayer hydrate. Bulk proton transport occurs through these layers, with a conductivity of $(8 \pm 4) \times 10^{-6}$ ohm^{-1}cm^{-1} at 20°C. Upon heating to 55°C, 0.5 H_2O per formula was gradually lost, but the conductivity was essentially retained. Upon further heating to 62°C another 0.5 H_2O was rapidly lost, resulting in a conductivity drop of a factor of 10. Further water was gradually lost until HTi_2NbO_7 was reached at 220°C. The X-ray evidence revealed no discrete, fixed-composition hydrate phases, indicating a single isostructural phase from $HTi_2NbO_7 \cdot 2H_2O$ to HTi_2NbO_7, with a single continuously variable interlayer spacing. The bulk conductivity of $CsTi_2NbO_7$ was less than 10^{-8} ohm^{-1}cm^{-1}.

Introduction

The magnitude and mechanism of proton conduction in layered acid hydrates varies considerably among the few examples so far investigated. High bulk conductivity of 4×10^{-3} ohm^{-1}cm^{-1} at 17°C is exhibited by $HUO_2PO_4 \cdot 4H_2O$ (*1*). The H-montmorillonite hydrates exhibit high proton conductivity (10^{-4} to 10^{-2} ohm^{-1}cm^{-1} at 20°C) of a mixed bulk and interparticle character (*2*). In contrast, $Zr(HPO_4)_2 \cdot H_2O$ possesses a bulk conductivity below 10^{-8} ohm^{-1}cm^{-1} at room temperature (*3*), although the surface conductivity is in the region of 10^{-5} ohm^{-1}cm^{-1} at 20°C (*4*), and the conductivity of wet pellets, arising from interparticle conductivity, extends almost to 10^{-2} ohm^{-1}cm^{-1} at 20°C (*3*). Recently the new layered acid hydrate $HTi_2NbO_7 \cdot 2H_2O$ was prepared (*5*), and was formulated as $H_3OTi_2NbO_7 \cdot H_2O$ (*5*). Since this compound affords another example of a layered acid hydrate, we have investigated the magnitude and mechanism of the anticipated proton conductivity, and have also characterized and determined the conductivity of the lower hydrates. The conductivity of $CsTi_2NbO_7$, from which $HTi_2NbO_7 \cdot 2H_2O$ was prepared by ion exchange, was also investigated for comparison.

The structure of both the Cs and H forms is built up from layers containing zigzag strings containing groups of 3 edge-shared octahedra. The strings are linked side by

* Present address: Materials Research Center, Coxe Laboratory #32, Lehigh University, Bethlehem, Pa. 18015.

† Present address: Amoco Research Center, P.O. Box 400, Naperville, Il. 60566.

0022-4596/84 $3.00

side via corner sharing to form $Ti_2NbO_7^-$ layers (*5*). The Cs ions occupy distorted cubic sites between the layers. No hydrates of the Cs salt are known. Three isomorphous acid salts have been reported (*5*). In the case of HTi_2NbO_7 and $HTi_2NbO_7 \cdot H_2O$, the interlayer spacing, given by half the *b* unit cell parameter, is smaller than in the Cs salt, whereas in $HTi_2NbO_7 \cdot 2H_2O$ the layers are separated more than in the Cs salt. Atomic positions for the hydrogens are not available for these compounds. However, deuterium positions have been identified in the related layer compound $DTiNbO_5$ (*6*), in which the triply coupled octahedra found in HTi_2NbO_7 are replaced by doubly coupled octahedra. The deuteriums formed hydrogen bonds between two oxygens, one from each of the adjacent $TiNbO_5^-$ layers, and the proton conductivity was less than 10^{-8} $ohm^{-1}cm^{-1}$ at room temperature (*6*). Hydrates of this material, in which the proton conductivity would be expected to be considerably enhanced, have, however, not been found (*6*).

Experimental

$CsTi_2NbO_7$ was prepared from A.R. reagents by firing a mixture of $CsNO_3$, TiO_2, and Nb_2O_5 as previously described (*7*), and the known structure (*7*) was confirmed by X-ray diffraction. Following Rebbah *et al.* (*5*), $HTi_2NbO_7 \cdot 2H_2O$ was prepared by ion exchange of 5 g $CsTi_2NbO_7$ powder with 1-liter batches of 6 *N* HCl stirred and exchanged every day for 7 days. The product was washed with distilled water and dried in air. Samples for conductivity measurements were washed with distilled water until the conductivity of the wash liquid was 10^{-5} $ohm^{-1}cm^{-1}$. The following X-ray lattice parameters agreed well with the reported values (*5*), given in parentheses: a = 9.26 (9.296) Å, b = 21.1 (21.04) Å, and c = 3.78 (3.768) Å. There was no trace of the well-differentiated (020) peak of the Cs salt, corresponding to a smaller b parameter of 18.41 Å (*5*). Atomic absorption analysis for Cs showed 0.7 and 0.8% Cs for two samples, corresponding to an average of 98% exchange of Cs with H. Water contents were determined thermogravimetrically by heating to 1000°C. The Cs compound lost a weight equivalent to 0.09 waters per formula, while the weight loss for the hydrogen compound indicated the formula $HTi_2NbO_7 \cdot 1.97H_2O$, averaged over two runs.

X-Ray parameters were obtained using Cu radiation and a Philips 1050/25 powder diffractometer fitted with a hot stage. Thermogravimetric and differential thermal analysis were performed on a Stanton Redcroft STA780 microbalance instrument using 20- to 50-mg samples with the thermal capacity reference pan empty. Laboratory air was passed over the samples at 50 ml min^{-1}. The weights were corrected for the small effect of the gas flow as a function of temperature. Conductivity measurements were made either at a pressure of 2 ton cm^{-2} (20 MPa), using stainless-steel plungers in a plastic die (*8*), or under strong spring pressure in a high-temperature rig with silver plungers (*9*). Conductivities were determined at either 1592 Hz using a Wayne Kerr bridge B624 or from 100 Hz to 60 kHz using a B224 bridge. The complex impedance plot was obtained on selected samples using a Solartron impedance analyzer by courtesy of Professor R. J. Brook of the Ceramics Dept. In all cases only a single semicircle with a sloping low frequency line was observed, and the extrapolated intercept gave a conductivity typically about 30% lower than the value obtained at 1592 Hz. Since this is less than the observed variation from sample to sample caused by the effects of temperature, humidity level, and densification processes over a period of time under pressure, we have quoted the normally measured values obtained at 1592 Hz.

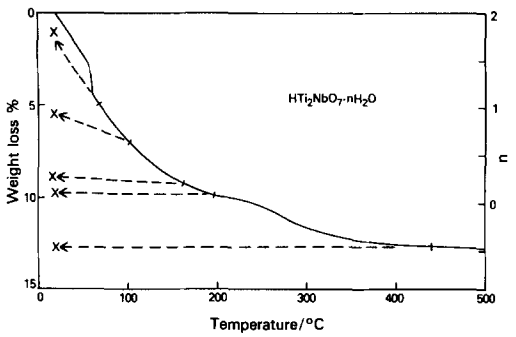

FIG. 1. TGA curve for $HTi_2NbO_7 \cdot 2H_2O$, heated at 0.1°C min^{-1}. No further detectable weight loss occurred upon heating from 500 to 1000°C, at 5°C min^{-1}. Cooling thermograms, each for a separate sample, are indicated by the dashed lines, and indicate the degree of reversibility of the dehydration.

Results

Thermogravimetric Analysis

Figure 1 shows the TGA curve for $HTi_2NbO_7 \cdot 2H_2O$, performed at the very slow heating rate of 0.1°C min^{-1} in order to achieve near-equilibrium between the sample and the water vapor partial pressure of the purging laboratory air (*10*). It can be seen that the sample began losing weight as soon as the temperature was raised above room temperature. However, no further weight gain was detected upon lowering the temperature from 21 to 17°C by chilling the furnace cooling water. Furthermore, there was no change in the interlayer spacing, given by half the *b* unit cell parameter, when an X-ray sample was moistened with water. We conclude that the maximum hydrate, namely $HTi_2NbO_7 \cdot 2H_2O$, is essentially obtained at equilibrium in air at room temperature, in agreement with the formula of $HTi_2NbO_7 \cdot 1.98H_2O$ and $HTi_2NbO_7 \cdot 1.95H_2O$ as obtained from the weight loss obtained after heating two separate samples to 1000°C.

The TGA curve, shown in Fig. 1, shows a sharp transition between 56 and 62°C, centered about 59°C, and a slight plateau at 220°C. The losses from 21 to 62°C, and from 62 to 220°C correspond, respectively, to the loss of 0.94 H_2O and a further 0.94 H_2O, indicating the following dehydration sequence:

$$HTi_2NbO_7 \cdot 2H_2O \xrightarrow[-H_2O]{21\text{–}62^\circ C} HTi_2NbO_7 \cdot H_2O \xrightarrow[-H_2O]{62\text{–}220^\circ C}$$

$$HTi_2NbO_7 \xrightarrow[-\frac{1}{2}H_2O]{220\text{–}460^\circ C} \text{oxides}$$

At heating rates of 1 and 2°C min^{-1} the center of the sudden weight loss shifted to 71 and 110°C, respectively, and the endpoint of the transition became poorly defined. Rebbah *et al.* (*5*) reported the first water loss between 90 and 100°C, and the second between 100 and 390°C. The lower temperatures obtained at a heating rate of 0.1°C min^{-1} in this study can be taken as representing more closely the true thermodynamic temperatures. A structural explanation for the interesting gradual then rapid two-stage loss of the first water per formula will be advanced in the Discussion section.

The reversibility of the transitions was investigated by cooling a range of samples down to room temperature after equilibration in the TGA unit at a given elevated temperature. The time independent room temperature compositions of these samples are shown in Fig. 1. It can be seen that complete rehydration never occurs, and the extent of rehydration diminishes at higher temperatures until at 200°C, at the composition HTi_2NbO_7, no water was regained upon cooling. The cooled samples were further investigated by means of ir spectroscopy and X-ray diffraction.

Infrared Spectra

The ir spectra of $HTi_2NbO_7 \cdot 2H_2O$, obtained using a Nujol mull between KCl disks, showed a broad absorption between 3200 and 3600 cm^{-1}, assigned to the stretch-

ing modes of water; a sharp peak at 1620 cm^{-1} assigned to the bending mode of water; and two sharp peaks at 960 and 910 cm^{-1} superimposed on a broad absorption extending between 1000 and 400 cm^{-1}, assigned to metal–oxygen group vibrations. The peaks at 960 and 910 cm^{-1} could either be bending modes of *M*–OH groups, or further metal–oxygen group vibrations. Deuterium substitution experiments would be needed to indicate a definite assignment. There was no absorption in the region of 1150 or 1750 cm^{-1}, characteristic of H_3O^+ groups, as clearly evident in the ir spectrum of $HUO_2PO_4 \cdot 4H_2O$ (*11*). However, this does not necessarily indicate the absence of H_3O^+ groups, since the bands may be washed out by molecular motion or a range of local symmetries.

The ir spectra of the partially dehydrated samples prepared by heating, as described above, showed that the 3200- to 3600-cm^{-1} band occurred only when *n* in the formula $HTi_2NbO_7 \cdot nH_2O$ lay between 1 and 2 in the samples at room temperature, and that the absorption at 1620 cm^{-1} occurred for *n* between 0 and 2, and that the peak at 960 cm^{-1} only disappeared after complete decomposition to the oxides.

X-Ray Diffraction

Diffractograms were obtained in two ways. A powdered sample of $HTi_2NbO_7 \cdot 2H_2O$ was heated to various temperatures in air on the hot stage of the X-ray camera, allowed to equilibrate for several hours and the diffractogram recorded. The sample holder was an aluminum plate with a trough cut out, and the sample was leveled off carefully to ensure the correct height so that low-angle measurements to determine the *b* parameter could be accurately made. The results at the various temperatures are shown in Fig. 2. All samples retained the orthorhombic unit cell, as previously found (*5*).

The second type of experiment involved obtaining the diffractograms of the samples which had been heated in the TGA unit and cooled back to room temperature, as previously described. The *b* unit cell parameters were consistent with those obtained under equilibrium conditions if allowance was made for rehydration.

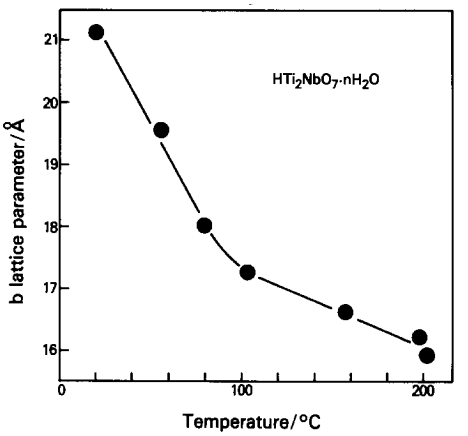

FIG. 2. Lattice parameter, *b*, perpendicular to the layers, for $HTi_2NbO_7 \cdot 2H_2O$ and its dehydration products, determined at the indicated temperatures.

None of the diffractograms showed two 020 peaks, from which the *b* parameter was determined, and the gradual but large shifts in the Bragg angle with dehydration clearly indicated that only one phase was ever present. The widths of the peaks for all the dehydrated samples were nevertheless about twice that of the sharp peak of the initial compound, but the widths were small compared to the large Bragg angle changes.

Ionic Conductivity

Table I gives the conductivities obtained for $HTi_2NbO_7 \cdot 2H_2O$ and $CsTi_2NbO_7$, measured under 2 ton cm^{-2} pressure applied via stainless-steel plungers in a Perspex die. The conductivities of selected samples were not significantly different when measured in a special die (*8*) in which the applied voltage was perpendicular to the direction of the applied pressure, and thus parallel to the layers. Hence, even

TABLE I

CONDUCTIVITIES, IN $ohm^{-1}cm^{-1}$ AT 17 TO 21°C, OF PRESSED PELLETS, AS A FUNCTION OF CONDITIONS

		Pressed powders	
	Pressed pastes	Initial	Final, after several days
$HTi_2NbO_7 \cdot 2H_2O$	$(2 \pm 1) \times 10^{-4}$	$(9 \pm 3) \times 10^{-5}$	$(8 \pm 4) \times 10^{-6}$
$CsTi_2NbO_7$	$(4 \pm 1) \times 10^{-4}$	$(2 \pm 1) \times 10^{-5}$	$(2 \pm 1) \times 10^{-5}$

though the particles may have had a platelike shape, there was no distinct conduction anisotropy in the pressed pellets.

The pressed pastes were made by compaction of powders which had been moistened with distilled water. Samples dried in air at room temperature gave lower conductivities, as indicated in the table, and further water loss from the H-form appeared to occur under a constant applied pressure, as inferred from the tabulated conductivity reduction. The effect of time, or an increase in pressure from 2 to 10 ton cm^{-2} was, however, only marginal in the case of pressed pastes in which a constant water content was maintained by keeping a small amount of water around the plunger. The errors indicated in the table cover the spread of values obtained from a number of measurements.

A second set of measurements, shown in Fig. 3, was made using the high-temperature rig. The values have been normalized so that the initial values agree with those obtained as described above at 2 ton cm^{-2} pressure, for which good compaction was obtained compared to the thumbscrew pressure attained in the high-temperature rig. A correction factor of 3 was used for all samples. As can be seen, the pronounced drop in the conductivity of the Cs form when heated to 30°C contrasts with the sustained conductivity of the H-form. The mechanistic implications of these results are presented below.

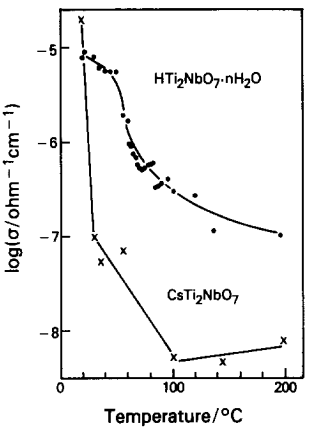

FIG. 3. Conductivity of $HTi_2NbO_7 \cdot 2H_2O$ and its dehydration products, and of $CsTi_2NbO_7$, as a function of temperature. Each point represents the equilibrium conductivity obtained typically after 24 hr at constant temperature.

Discussion

The combination of the above measurements provides the following detailed description of these layered hydrates. The dependence of the interlayer spacing on water content, as presented in Fig. 4, clearly shows that the spacing increases by approximately 2.6 Å per water molecule in the formula. Since the *b* parameter encompasses two oxide layers and two hydration layers, each hydration layer expands by 1.3 Å in going from HTi_2NbO_7 to $HTi_2NbO_7 \cdot H_2O$, and by another 1.3 Å when $HTi_2NbO_7 \cdot 2H_2O$ is formed. This increment is roughly half the value of 2.8 Å per

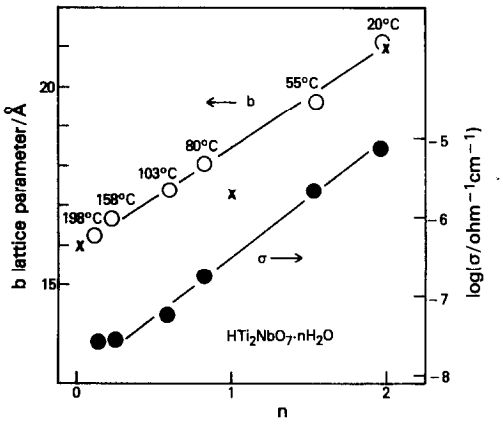

FIG. 4. Variation of interlayer spacing (open circles), and conductivity (full circles) of $HTi_2NbO_7 \cdot nH_2O$ as a function of water content n. The errors are within the circle sizes. The parameters were all determined at equilibrium at the temperatures indicated. The effect of thermal expansion alone on the interlayer spacing was found to be less than 0.3 Å between 20 and 200°C, which is small compared to the changes due to dehydration. The b parameters from Ref. (*5*) are given by the crosses.

water layer found for the mono-, di-, and tri-hydrates of montmorillonite (*12*). In these hydrates, the water molecules have considerable mobility and form an expanded and randomized hydrogen-bond network. However, in the topic hydrates, the spacing data indicates a close-packed arrangement of the waters to the oxide ions of the structural layers. The results are thus consistent with $HTi_2NbO_7 \cdot H_2O$ having one water layer between the oxide sheets, in which the water molecules probably occupy the same sites as Cs in $CsTi_2NbO_7$. Additional waters cause further lattice expansion to form a second water layer in $HTi_2NbO_7 \cdot 2H_2O$. The exact determination of the water positions will have to await detailed diffraction experiments. A similar set of relationships to those depicted in Fig. 4 was found also for the room temperature parameters of the set of samples which had been cooled to room temperature after heating.

Turning to the structural evolution during dehydration, the observation of only a single phase at any given temperature coupled with the monotonic dependence of the b parameter as a function of water content, as seen in Fig. 4, is in contrast with the expected two-phase behavior, as seen, for instance, during the gradual dehydration of the bilayer montmorillonite hydrates to the monolayer hydrates (*12*). The following mechanism is proposed. Rather than water loss occurring uniformly from each layer, which would result in stepwise dimensional changes, water loss occurs preferentially from certain layers to give, within one crystal, a mixture of, for instance, bilayers and monolayers. These are intermixed so as to give a continuously variable average layer separation, as actually found. The TGA curve shown in Fig. 1 shows a gradual water loss from $HTi_2NbO_7 \cdot 2H_2O$ until the average composition $HTi_2NbO_7 \cdot 1.5H_2O$ is reached. Rather than having only half-filled layers, this would correspond, in the model proposed, to an equal number of completely filled monolayers and completely filled bilayers. Rapid loss of water then follows to produce only the monolayer structure of $HTi_2NbO_7 \cdot H_2O$.

Normally, during the dehydration of layer hydrates, two X-ray peaks are present representing the two layer thicknesses of the two phases in equilibrium, and the constant position of these peaks enables the lattice parameters of the two phases to be accurately determined, as in the montmorillonite clays. However, with a continually changing lattice parameter as in $HTi_2NbO_7 \cdot nH_2O$, the lattice parameter when $n = 1$ can only be obtained at the temperature for which $n = 1$. Rebbah *et al.* (*5*) found this temperature to be between 90 and 100°C, and determined b for $HTi_2NbO_7 \cdot H_2O$ in this region to be 17.17 Å, as shown by the cross in Fig. 4 for $n = 1$. As can be seen from the other two crosses in Fig. 4., there is good agreement for the b parameters of the end members having $n = 0$ and 2. Our

slower TGA measurement showed a lower temperature of 62°C for which $n = 1$. From Fig. 4, $b = 18.50$ Å when $n = 1$, from our data, and we believe this to be a more accurate value for $HTi_2NbO_7 \cdot H_2O$.

Our improved value of b for $HTi_2NbO_7 \cdot H_2O$ now reflects in the comparison with the alkali metal forms MTi_2NbO_7. The values of Rebbah *et al.* (*5*) indicated that the b parameters of $HTi_2NbO_7 \cdot H_2O$ and $K_{0.85}H_{0.15}Ti_2NbO_7 \cdot 0.15H_2O$ were almost identical. Because of the similarity in the ionic radii of K^+ and H_3O^+, this evidence was used to support the formulation (*5*) $H_3OTi_2NbO_7$. However, our significantly larger value for b for this compound now exceeds that even for $CsTi_2NbO_7$ of 18.41 Å (*5*), thus invalidating the quoted evidence (*5*) for the presence of H_3O^+ ions.

Let us now consider the conductivity in the light of the structural features deduced above. Three conductivity mechanisms can be identified: voidal solution conductivity, surface conductivity, and bulk conductivity.

First, voidal solution conductivity is evident from the following features. The conductivity of both $CsTi_2NbO_7$ and $HTi_2NbO_7 \cdot 2H_2O$ was roughly 10 times higher when measured on pressed pastes as compared to dry powders, indicating some donation of Cs^+ or H^+ ions from the particles into the aqueous solution filling the voidal network within the pellet. Such a donation of the exchangeable ion into the voidal solution to enhance the conductivity was also found for a range of zeolites (*13*), and depends on the ease of donation of the surface exchangeable cations.

Second, surface conductivity is found in the dry Cs form at room temperatures and is revealed by comparing the behavior of the Cs and H salts, as shown in Fig. 3. The drop in the conductivity of the Cs salt of more than a factor of 100 upon heating to 30°C clearly indicates that the room temperature conductivity was surface conductivity caused by the presence of an equilibrium quantity of adsorbed or condensed surface water into which free exchangeable cations had been donated. Heating to 30°C apparently removes most of the surface water, thereby removing the conduction medium. The further drop in the conductivity at 100°C, as seen in Fig. 3, indicates that the true bulk conductivity of the Cs form is probably below 10^{-8} $ohm^{-1}cm^{-1}$ at room temperature.

Third, bulk conductivity is found in the dry H form, as deduced from the following. In contrast to the behavior of the Cs form, the conductivity of the H form remained approximately constant when held for long periods between room temperature and 50°C, where there would be a negligible influence from surface water. At higher temperatures, comparison of Figs. 1 and 3 shows that the loss of crystalline water of hydration between 52 and 62°C is accompanied by a pronounced drop in the conductivity. Both of these factors indicate that the conductivity is a bulk phenomenon occurring within the hydration layers of the compound. Even at room temperature the bulk conductivity is higher or as high as the expected surface conductivity arising from surface moisture.

Considering the very low bulk conductivity of the Cs compound, and the 98% exchange of H^+ for Cs^+ achieved in the preparation, we attribute the conductivity of the H-form to protonic conduction. Any electronic conductivity would derive from the $Ti_2NbO_7^-$ layers. Since the observed conductivity of the Cs form is less than 10^{-8} $ohm^{-1}cm^{-1}$ above 100°C this must represent an upper limit on the magnitude of the electronic conductivity, not only in the Cs form, but probably also in the H form as well. In any case, the electronic conductivity of the H-form would not be more than the value of 10^{-7} $ohm^{-1}cm^{-1}$ found for the total conductivity of the H-form at 200°C. This only represents a maximum of 1% of

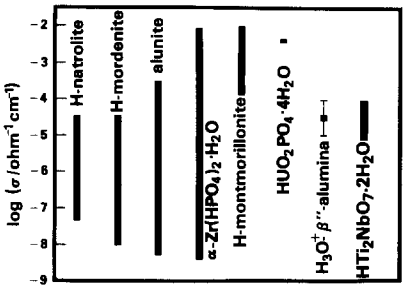

FIG. 5. Room temperature conductivities of a range of proton conductors. The tops of the bars correspond to wet pressed pellets, while the bottoms of the bars correspond to samples equilibrated in air.

the room temperature conductivity, thus indicating almost exclusive ionic conduction for the acid hydrates.

Regarding the position of the exchangeable protons in $HTi_2NbO_7 \cdot 2H_2O$, we have shown that, contrary to previously claimed (*5*), the structural evidence does not substantiate the presence of H_3O^+. Neither is there any confirmation of this species from our ir studies. The attachment of the proton to the oxide framework, represented as $Ti_2NbO_6OH \cdot 2H_2O$, is equally plausible on chemical grounds to the presence of H_3O^+. However, at present there exists no definite evidence one way or the other. The bulk conductivity would be consistent with either formulation. In the case of $Ti_2NbO_6OH \cdot 2H_2O$, partial dissociation of the *M*–OH groups would produce a small concentration of H_3O^+ ions in the water layers. In the case of $H_3OTi_2NbO_7 \cdot H_2O$, there would be a much higher concentration of charge carriers in the layers, and a lower mobility could be tolerated. In both cases the proton transport would occur via the Grotthus mechanism by proton transfer between H_3O^+ and H_2O. As is evident from Figs. 3 and 4, the conductivity progressively declines as the water content diminishes, in accord with the above mechanism.

Finally, a comparison of the proton conductivity of $HTi_2NbO_7 \cdot 2H_2O$ with a range of other proton conductors (*13*) is shown in Fig. 5. The spread in conductivity from wet to dry conditions in the case of $HTi_2NbO_7 \cdot 2H_2O$ is relatively small, and reflects the appreciable bulk conductivity exhibited by this compound, which is considerably higher than the bulk conductivity of many of the other compounds, which is equivalent to or smaller than the bottom of the bars. As described in the introduction, a range of conduction mechanisms is found for these compounds. $HTi_2NbO_7 \cdot 2H_2O$ is distinguished by the stability of the conductivity up to 50°C in air. Apart from $HUO_2PO_4 \cdot 4H_2O$, which retains its conductivity also up to about 50°C in air, and H_3O–β''-alumina, which retains its conductivity up to even higher temperatures, all the other compounds in Fig. 5 have rapidly declining conductivities above room temperature due to loss of bulk or surface water.

Acknowledgment

One of us, M. L., thanks the Science Research Council for a Post Doctoral Fellowship.

References

1. M. G. SHILTON AND A. T. HOWE, *Mater. Res. Bull.* **12,** 701 (1977).
2. S. H. SHEFFIELD AND A. T. HOWE, *Mater. Res. Bull.* **14,** 929 (1979).
3. G. ALBERTI, M. CASCIOLA, U. CONSTANTINO, AND R. RADI, *Gazz. Chim. Ital.* **109,** 421 (1979).
4. E. KROUGH ANDERSEN, I. G. KROGH ANDERSEN, C. KNAKKERGARD MOLLER, K. E. SIMONSENAND, AND E. SKOU, *Solid State Ionics* **7,** 301 (1982).
5. H. REBBAH, M. HERVIEU, AND B. RAVEAU, *Mater. Res. Bull. 16,* 149 (1981).
6. H. REBBAH, J. PANNETIER, AND B. RAVEAU, *J. Solid State Chem.* **41,** 57 (1982).
7. M. HERVIEU AND B. RAVEAU, *J. Solid State Chem.* **32,** 161 (1980).

8. P. E. CHILDS, A. T. HOWE, AND M. G. SHILTON, *J. Solid State Chem.* **34,** 341 (1980).
9. C. M. JOHNSON, M. G. SHILTON, AND A. T. HOWE, *J. Solid State Chem.* **37,** 37 (1981).
10. A. T. HOWE AND M. G. SHILTON, *J. Solid State Chem.* **31,** 393 (1980).
11. M. G. SHILTON AND A. T. HOWE, *J. Solid State Chem.* **34,** 137 (1980).
12. W. F. BRADLEY, R. E. GRIMAND, AND G. L. CLARK, *Z. Kristallogr.* **97,** 216 (1937).
13. M. LAL, C. M. JOHNSON, AND A. T. HOWE, *Solid State Ionics* **5,** 451 (1981).